N O T I C E

THIS DOCUMENT HAS BEEN REPRODUCED FROM
MICROFICHE. ALTHOUGH IT IS RECOGNIZED THAT
CERTAIN PORTIONS ARE ILLEGIBLE, IT IS BEING RELEASED
IN THE INTEREST OF MAKING AVAILABLE AS MUCH
INFORMATION AS POSSIBLE

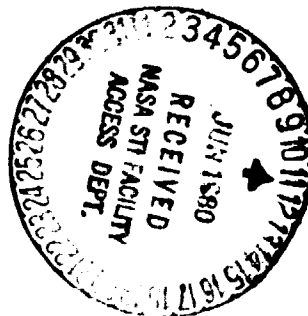# Comparison of the Nimbus-4 BUV Ozone Data with the Ames Two-Dimensional Model

W. J. Borucki and I. J. Eberstein

May 1980

Comparison of the Nimbus-4 BUV Ozone Data with the Ames Two-Dimensional Model

W. J. Borucki, Ames Research Center, Moffett Field, California
I. J. Eberstein, Goddard Space Flight Center, Greenbelt, Maryland

Comparison of the Nimbus-4 BUV Ozone Data

With the Ames Two-Dimensional Model

By W. J. Borucki[1]) and I. J. Eberstein[2])

Abstract — A comparison is made of the first two years of Nimbus-4 backscattered ultraviolet (BUV) ozone measurements with the predictions of the Ames two-dimensional model. The ozone observations used in this study consist of the mixing ratio on the 1-, 2-, 5-, and 10-mb pressure surfaces. These data are zone and time averaged to obtain seasonal means for 1970 and 1971 and are found to show strong and repeatable meridional and seasonal dependencies. The model used for comparison with the observations extends from 80° N to 80° S latitude and from altitudes of 0 to 60 km with 5° horizontal grid spacing and 2.5-km vertical grid spacing. The chemical reaction and photolysis rate constants used in the model are those recommended in the report of the NASA Panel for Data Evaluation (1979). Chemical reaction and photolysis rates are diurnally averaged, and the photodissociation rates are corrected for the effects of scattering.

It is found that the large altitude, latitude, and seasonal changes in the ozone data agree well with the model predictions. Also shown are model predictions of the sensitivity of the comparisons to changes in the assumed mixing ratios of water vapor, odd nitrogen, and odd chlorine, as well as to changes in the ambient temperature and transport parameters.

Key words: Ozone; Stratosphere; Nimbus-4

[1]) NASA-Ames Research Center, Moffett Field, California, 94035.

[2]) NASA-Goddard Space Flight Center, Greenbelt, Maryland, 20771.

1. Introduction

Because ozone affects the solar UV radiation that reaches the earth's surface and because ozone influences stratospheric circulation patterns, it is important to determine the global distribution of ozone and to understand the mechanisms that control the ozone distribution.

Model predictions of the variation of the ozone distribution with altitude, latitude, and season allow us to comprehend the mechanisms that control the production, loss, and movement of ozone. Hence, it is important to continuously compare model predictions with the measured distributions over as wide a range of conditions as possible to assess the depth of our understanding of these mechanisms and the validity of our predictions of the effects of anthropomorphic disturbances.

As so often happens, the easiest measurements to make have been precisely the one that are the most difficult to model, i.e., measurements at one point in space and time. However, with the advent of satellite measurements of ozone by HEATH et al. (1973) and PRABHAKARA et al. (1973), measurements of ozone distributions became available that are much more representative of seasonal and meridional means and are thus more amenable to comparisons with currently available models. These measurements are not yet completely satisfactory in that the BUV (backscattered ultraviolet) measurements do not cover the winter pole and the IRIS measurements do not give the vertical distributions of ozone. Further, these measurements are not entirely consistent and they suffer from problems associated with mathematical difficulties in deconvolving the measurements to obtain the vertical distributions. Finally, the satellite data are available only for fairly short periods of time and hence might not be representative of long-term means. Nevertheless, the

ORIGINAL PAGE IS OF POOR QUALITY

satellite data offer a significant improvement over previous data in that their internal consistency and large geographical coverage allow a more realistic determination of the vertical, meridional, and seasonal distributions of ozone for comparison with model predictions.

It is the purpose of this paper to compare the Ames two-dimensional model predictions of ozone concentrations with the BUV observations from the Nimbus-4 satellite and to interpret the comparisons. Such a comparison should be viewed as an early attempt at model validation. As satellite data on other minor constituents (such as oxides of nitrogen, hydroxyl, and halogens) become available, it will become possible to make more complete, and thus more sophisticated, comparisons.

2. *Nimbus IV BUV Experiment*

The BUV experiment is on the Nimbus-4 satellite, which was launched into a circular polar orbit at an altitude of 1100 km. The 10° retrograde orbit is sun synchronous, and every 107 minutes the three-axis-stabilized satellite passes through the ascending node near local noon. The subsatellite point crosses the equator in increments of 27° in longitude between successive passes and reaches a maximum latitude of 80°. The spatial resolution of the instrument is 230 km, or approximately 2° latitude (HEATH et al., 1973).

The instrument is a double (tandem) Ebert-Fastie spectrophotometer in conjunction with a narrow band interference filter photometer (HEATH et al., 1973). The spectrometer is designed to measure spectral intensities at twelve wavelengths between 255.5 nm and 339.8 nm with a 1-nm bandpass. The resulting light intensity is measured with a high-quantum-efficiency photomultiplier tube. The absolute error of the intensity measurement is estimated at ±10% while the relative error is only 2% to 5% (FLEIG, 1980; HEATH et al., 1979).

3

The principle of the BUV experiment rests on the fact that atmospheric radiance at a particular wavelength originates in a moderately well-defined effective scattering layer. An outline of the principle of the experiment can be deduced from Fig. 1. The intensity of light reaching the observing instrument is proportional to the molecular density in the scattering layer. By using the hydrostatic equation and the ideal gas law it is readily shown that absorption by ozone along the path shown in Fig. 1 is proportional to the pressure at the scattering level.

Thus, we have the light reaching the receiver given by the following relation of proportionality

$$I = B\left(1 - Y_{O_3}\sigma_\lambda P\right)(\beta_\lambda P) \qquad (1)$$

where σ_λ = ozone absorption coefficient

Y_{O_3} = mean ozone mixing ratio along the optical path

β_λ = scattering cross section

P = pressure

The parameter B is a constant of proportionality. It may seen from equation (1) that I goes to zero at the top of the atmosphere, where $P = 0$, and at the "bottom" defined by maximum penetration depth, wher $1 - Y_{O_3}\sigma P = 0$. Between those extremes, I must go through a maximal value, whose position may be found by differentiating equation (1) with respect to P and setting the derivative equal to zero. The pressure corresponding to maximum intensity is thus given by

$$P_{I_{max}} = \frac{1}{2Y_{O_3}\sigma_\lambda} \qquad (2)$$

It may be seen from equation (2) that the height of the maximum of the contribution function depends on the ozone absorption coefficient at the

4

wavelength λ and on the amount of ozone present. A set of representative weighting functions is shown in Fig. 2.

3. BUV Data Reduction

Following TWOMEY (1961) and MATEER (1972) we may write the expression for the backscatter radiance as follows:

$$I(\lambda,\theta) = F_0(\lambda)\left(\frac{3\beta_\lambda}{16\pi}\right)(1 + \cos^2\theta)S(\bar{\nu}, X_p) \tag{3a}$$

$$S(\bar{\nu},X_p) = \int_0^1 \exp[-(1 + \sec\theta)(\alpha_\lambda X_p + \beta_\lambda P)]dP \tag{3b}$$

where
I = backscattered radiance in the satellite nadir direction

θ = solar zenith angle

λ = wavelength of radiation

$\bar{\nu}$ = the wave number, $1/\lambda$

$F_0(\lambda)$ = extraterrestrial solar irradiance

β_λ = atmospheric scattering coefficient

α_λ = ozone absorption coefficient

X_p = ozone column density above pressure P

In equation (3) a plane parallel atmosphere has been assumed. Thus, additional correction terms are needed for high solar zenith angles.

In the upper stratosphere, absorption by ozone is much stronger than Rayleigh scattering, and thus the scattering term $\beta_\lambda P$ may be neglected compared with the absorption term $\alpha_\lambda X_p$.

5

Equation (3b) may thus be rewritten as follows:

$$S(\bar{v}, X_p) = \int_0^1 [\exp(-kX_p)]dP \tag{3c}$$

where the pressure independent terms have been gathered in the quantity

$$k \equiv \alpha_\lambda (1 + \sec \theta)$$

Following TWOMEY (1961), the ozone column density, X_p, can be made into the variable of integration. Thus the right side of equation (3c) the Laplace transform of the derivative of P with respect to X_p. Assuming the $P(X_p)$ is bounded by an exponential less than $\exp(kX_p)$, equation (3c) now becomes

$$S(\bar{v}, X_p) \equiv Q(k) = kL[P(X_p)] \tag{4}$$

Since $S(\bar{v}, X_p)$ is a measured quantity, equation (4a) can be solved provided that one can find a relationship between P and X_p. GREEN (1964) suggested the following:

$$X_p = CP^{1/\sigma} \tag{5a}$$

$$P = C^{-\sigma} X_p^{\sigma} \tag{5b}$$

where C and σ are empirical parameters to be determined from the data. It is readily seen from equation (5) that σ is the ratio of ozone scale height to atmospheric scale height. This ratio is now assumed to be constant in the upper stratosphere. Substituting equation (5b) into equation (4) and taking the inverse transform (CHURCHILL, 1958, p. 324) yields the following expression:

$$Q(k) = (Ck)^{-\sigma} \Gamma(\sigma + 1) \tag{6}$$

6

The four shortest wavelengths of the experiment are now used to draw a straight line with slope $-\sigma$ on a log-log plot, giving ozone overburden as a function of atmospheric pressure. Differentiating the result gives ozone mixing ratio. The above inversion may be used for atmospheric pressures less than 2 to 3 mb, i.e., altitudes above 45 km. For larger pressure levels, or lower altitudes, the assumption that the loss of light intensity due to ozone absorption is much larger than that due to scattering can no longer be made, i.e., the $\beta_\lambda P$ term can no longer be neglected compared with $\alpha_\lambda X_p$. Thus, it becomes necessary to solve equation (3b) in its complete form, which cannot be done by the simple Laplace transform technique discussed above.

Now define

$$
\left.
\begin{array}{l}
\alpha_j \equiv (1 + \sec \theta)\alpha_\lambda \\[2mm]
\beta_j \equiv (1 + \sec \theta)\beta_\lambda
\end{array}
\right\}
\tag{7a}
$$

Then equation (3b) may be written in the form

$$
S_j(\bar{\nu}_j, X_p) = \int_0^1 e^{-\alpha_j X_p}\, e^{-\beta_j P}\, dP
\tag{7b}
$$

The term $S_j(\bar{\nu}_j, X_p)$ has been written in subscripted form since it is not a continuous function of frequency but is rather defined for a finite number of frequencies. Equation (7b) is a form of Fredholm's integral equation of the first kind (WHITTAKER and WATSON, 1958, p. 219), and it may be written as

$$
\phi(X) = \lambda \int_a^b K(X,\xi)\phi(\xi)d\xi
\tag{7c}
$$

7

FREDHOLM (1900) showed that the above integral equation is the limited form (when $\delta \to 0$) of the equation:

$$\phi(X_p) = \lambda\delta \sum_{q=1}^{n} K(X_p,X_q)\phi(X_q) \tag{8}$$

The above system of equations for $\phi(X_p)$ (p=1, 2...3) has a solution if the determinant formed by the coefficients of $\phi(X_p)$ vanishes. The expression for this determinant is given below from WHITTAKER and WATSON (1958).

$$D(\lambda) = \begin{vmatrix} 1 - \lambda\delta K(X_1,X_1) & - \lambda\delta K(X_1,X_2) & \cdots & - \lambda\delta K(X_1,X_n) \\ - \lambda\delta K(X_2,X_1) & 1 - \lambda\delta K(X_2,X_2) & \cdots & - \lambda\delta K(X_2,X_n) \\ \cdot & & & \cdot \\ \cdot & & & \cdot \\ \cdot & & & \\ - \lambda\delta K(X_n,X_1) & - \lambda\delta K(X_n,X_2) & \cdots & 1 - \lambda\delta K(X_n,X_n) \end{vmatrix} \tag{9}$$

Thus, the idealized problem reduces to finding eigen values of $D(\lambda)$. However, the real situation introduces special difficulties. Because of both noise in the experimental measurement and numerical inaccuracies, equation (9) cannot be solved exactly.

The implicit inversion problem now becomes one of minimizing the quantities:

$$\eta_j \equiv S_j - I_j \tag{10}$$

where S_j is the measured radiance at the jth wave number and I_j is the radiance obtained by assuming a specific ozone distribution. The quantity "j" varies over the number of wavelengths available for the experiment. In practice, j_{max} seldom exceeds 6 and is sometimes less; j_{max} limits the

8

information that can be recovered in the ozone profile to that represented by a polynomial of order j_{max}. A further difficulty is caused by numerical instabilities associated with the solution of equation (9). PHILLIPS (1962) has treated the case with numerical noise and developed a technique which is successful, but it imposes a smoothing constraint on the variation of X_p with P in equation (9). This approach was further refined by TWOMEY (1963).

In summary, the inversion procedure is as follows:

1. An initial guess of $X_p(P)$ is constructed from a spline fit of the solution of the Laplace solution for altitudes above 2 mb, and a mean atmospheric profile is obtained from rocket data for altitudes below 2 mb.

2. The backscatter equation (7b) is written in matrix form similar to equation (9) but incorporating the Phillips-Twomey smoothing parameter, γ.

3. The numerical profile of X_p as a function of P is put into matrix form, and the system is solved for the best profile consistent with experimental measurements.

The detailed numerical procedure will be available in report form from FLEIG, et al. (1980).

Analysis of the experiment indicates that the measurement error is between 2% and 5% (HEATH, et al., 1979). The inversion error ranges from 2% at a 50-km altitude to 5% at a 30-km altitude (FLEIG, personal communication, 1980). In addition, there is a sampling error of 1.5% to 2.5%, depending on the amount of data that was accepted for the calculation of the seasonal means. Combining these errors gives a total experimental error of 3% to 7.5%. A more complete analysis of the experimental errors can be obtained from the Goddard User's Manual for BUV Data by HUDSON et al. (1980).

4. Model description

The model is based on the governing equations for trace constituents

$$\frac{\partial n_i}{\partial t} + \nabla \cdot (n_i \mathbf{v}) + \nabla \cdot \boldsymbol{\phi}_i = S_i \tag{11}$$

$$\boldsymbol{\phi}_i = -\mathbf{K}_e \cdot \left[\nabla n_i + \left(\frac{1}{H} + \frac{1}{T}\frac{dT}{dz} \right) n_i \mathbf{e}_z \right] \tag{12}$$

where n_i = concentration of the ith constituent

ϕ_i = flux of the ith constituent

S_i = respective chemical production and loss rate term

H = atmospheric scale height

T = atmospheric scale temperature

$\mathbf{e}_z$ = vertical unit vector

$\mathbf{v}$ = bulk velocity of the atmosphere

$\mathbf{K}_e$ = eddy diffusivity tensor

The chemical rate equations are solved by using an implicit technique. Omitting the transport term from equation (11) yields the finite difference form:

$$\frac{n_i^{j+1} - n_i^{j}}{\Delta t} = S_i^{j+1} \tag{13}$$

which can be linearized by taking the first term in a Taylor series expansion of S_i^{j+1} about S_i^{j}:

$$\frac{n_i^{j+1} - n_i^{j}}{\Delta t} = S_i^{j} + \sum_k \frac{\partial S_i^{j}}{\partial n_k} \left(n_k^{j+1} - n_k^{j} \right) \tag{14}$$

10

The members of the set of mass conservation equations are coupled and require solution by matrix methods. With the implicit method, large time steps can be taken even though the equations are stiff.

The transport computations are time-split into those for vertical and horizontal advection and diffusion. Solutions for the transport processes are obtained from a mass-conserving, forward-time, space-centered, finite difference formulation of the equations. An implicit formulation is used for the horizontal diffusion and an explicit formulation is used for all other transport processes.

Spherical geometry is employed in equations (11) and (12) with the horizontal coordinate extending along a meridian from $80°$ S to $80°$ N in $5°$ intervals and the vertical coordinate extending from the ground to 60 km in 2.5-km intervals. End boundaries are taken at $80°$ S and $80°$ N because meridional fluxes are expected to be small at these latitudes. The end boundary conditions are taken to be zero flux of all constituents across the vertical boundaries. The upper boundary conditions are given by setting the vertical flux equal to zero for all species. The lower boundary condition for all species except HNO_3, N_2O, NO_2, O_3, HCl, H_2CO, and H_2O_2 is chemical equilibrium. Because HNO_3, H_2CO, HCl, and H_2O_2 are water soluble, fixed mixing ratios are imposed at the lower boundary that are consistent with the washout of these molecules in the troposphere. The number densities of NO_2 and N_2O are fixed at 3×10^9 cm^{-3} and $7.5 \times 10^{+12}$ cm^{-3}, respectively, at the lower boundary while the number density of O_3 is fixed at 6×10^{11} cm^{-3}. At each time step, the model calculates the concentrations of O_3, $O(^3P)$, $O(^1D)$, NO_2, NO, NO_3, N_2O, N_2O_5, HNO_3, HNO_2, H_2O_2, HO_2, N, OH, H, Cl, ClO, HCl, $ClNO_3$, CH_3, HCO, H_2CO, CH_3O_2, CH_3O, CH_4O_2, CO, CH_3Cl, $CFCl_3$, and CF_2Cl_2. The

profiles of N_2, O_2, H_2O, and H_2 are held fixed (at the experimentally determined values) during the calculations.

With a few exceptions, the values of the photochemical-reaction-rate constants that are used are those recommended in the report of the NASA Panel for Data Evaluation (1979) and are listed in the Appendix.

The chemical reaction and photolysis rates were diurnally averaged by using the techniques of TURCO and WHITTEN (1978) and COGLEY and BORUCKI (1976). The photodissociation rates have been corrected for the effects of scattering by a technique based on the work of LUTHER and GELINAS (1976).

The mean meridional circulation is obtained by the kinematic method from the steady-state equation of mass continuity in spherical coordinates:

$$\frac{1}{R \cos \theta} \frac{\partial}{\partial \theta} (\overline{\rho v} \cos \theta) + \frac{\partial}{\partial z} (\overline{\rho w}) = 0 \qquad (15)$$

where the overbar denotes a zonal and seasonal average

ρ = density

$\overline{v}$ = meridional velocity component

$\overline{w}$ = vertical velocity component

R = Earth's radius

θ = latitude

z = altitude above mean sea level

Equation (15) implies the existence of a "stream function" for the total flux such that

$$2\pi R \overline{\rho v} \cos \theta = - \frac{\partial}{\partial z} \Psi \qquad (16a)$$

$$2\pi R \overline{\rho w} \cos \theta = \frac{1}{R} \frac{\partial}{\partial \theta} \Psi \qquad (16b)$$

If the distributions of δ and $\bar{v}$ are known, $\bar{w}$ can be obtained from equation (16a) by vertical integration, and $\bar{w}$ can be obtained from equation (16b). The $\bar{v}$ components were based on the observed data of OORT and RASMUSSEN (1971) up to 20 km. Values of $\bar{v}$ based on observations are almost nonexistent above about 20 km. The observed $\bar{v}$ values were thus extrapolated to 60 km by the use of simple analytic functions that matched the 20-km values and could be adjusted until the mean circulation resembled that of other investigators, in particular that from the three-dimensional model of CUNNOLD, et al. (1975).

The eddy fluxes are parameterized by the eddy diffusion coefficients K_{yy}, K_{yz}, and K_{zz}. (The local "y-axis" is tangent to the meridian, i.e., $dy = Rd\theta$). The K values were obtained by trial and error until reasonable agreement was obtained between calculated and observed distributions of Carbon 14 (JOHNSTON et al., 1976) and the meridional distributions of the ozone column collated from reports of radiosonde observations by WILCOX et al. (1977). Except as otherwise noted, the eddy coefficients are those described in WHITTEN et al. (1977).

5. *Comparisons of the prediction and observations of the ozone distributions*

Figures 3 and 4 show the superposition of the BUV data (shown with ±10% error bars) and the model predictions for the four seasons. The dramatic changes in the latitude dependence of the data with pressure-altitude during a single season are evident. At pressure-altitudes of 1 and 2 mb, there is also a dramatic change of the latitude dependence with season. However, at 5 and 10 mb, the latitude dependence of the data is nearly independent of season. The model predictions of the changes in the latitude dependencies of the ozone abundances with season and with altitude agree well with the

observations. Although the agreement is good (note that linear rather than log scales are used in Figs. 3 and 4), there are discrepancies that are so much greater than the variability of the data that they require explanation. For example, the high-latitude predictions, particularly near the winter pole, are usually above the measurements. Although there is the possibility that the BUV experiment was somewhat less accurate at high latitudes because of the small amount of solar ultraviolet radiation to be backscattered and because of the obliqueness of the incoming radiation, it seems more likely that the model parameters that are used in the predictions are less certain at these latitudes.

To determine how the comparisons would be affected by other choices of atmospheric parameters that were assumed in the model or that were not well known, model runs were made for two temperatures and two choices of the mixing ratios of water vapor, odd chlorine and odd nitrogen. Two runs were also made to study the effects of changing the assumed transport parameters. The results of the parametric study are presented in the following sections.

Sensitivity of the comparisons to the assumed temperature fields

To determine the sensitivity of the comparison to the temperature uncertainties, the model temperatures were uniformly increased by 10°C at altitudes above 20 km and a new set of ozone predictions were generated. These predictions are plotted as dashed curves in Fig. 5. From this figure it can be seen that the predictions are lowered from 5% to 15%, depending on pressure height and latitude. In general, the increased temperatures cause the predictions to fall below the observations and lessen the agreement between the observations and predictions.

The temperature fields that are used in the model for altitudes above 20 km are derived from the rocket-data collation of NASTROM and BELMONT (1975); they represent long-term averages for each season. It is unlikely that seasonal-average temperatures that occurred during the 1969-1971 period differed by as much as 10°C from those used in our model. In fact, the temperature measurements made by the Selective Chopper Radiometer, which were reported by BARNETT (1974) for the period from November 1970 to November 1971 for pressure heights between 2 and 5 mb, are within ±3°C of those we used. If we assume that the temperatures in the stratosphere did not vary from those used in the model by more than ±3°C, then the effect of such a temperature uncertanity is less than ±5% at all latitudes and altitudes.

Sensitivity of the comparisons to the assumed water vapor abundance

The predicted ozone concentrations are sensitive to the amount of water vapor present because the water vapor reacts with $O(^1D)$ atoms to produce odd hydrogen species which catalytically destroy ozone at high altitudes. Unfortunately, zonally averaged water-vapor measurements are not available as a function of latitude and season for the 1969-1971 period of the BUV observations. Therefore, two different model assumptions about the amount of water vapor present were made to determine the sensitivity of the comparison to the range of water vapor likely to have been present during the observation period.

A collation of stratospheric measurements of H_2O at midlatitudes by HARRIES (1976) indicated that the average H_2O mixing ratio varied from 3 ppmv at 15 km to 5 ppmv at 45 km with an rms deviation of 1.5 ppvm. The H_2O measurements of HILSENRATH et al. (1977) show that the stratospheric water abundance is quite inhomogenous in that water-vapor mixing ratios as low as 1.6 ppmv and

as high as 13 ppmv were observed in their aircraft surveys between 70° N and 50° S latitude.

When the assumption of the water-vapor abundance in the model is changed from 4 ppmv to 8 ppmv, the model predicts a latitude-dependent ozone decrease that is most pronounced at the upper altitudes (See Fig. 6). The effect is greatest at low latitudes and varies from 3% at 5 mb to 15% at 1 mb pressure altitude.

Sensitivity of the comparisons to the assumed odd chlorine abundance

The effect on the predicted ozone profiles of the amount of odd chlorine (odd chlorine $\equiv$ Cl + HCl + ClO + ClNO$_3$) present is shown in Fig. 7. The solid curve shows the effects of assuming an asymptotic mixing ratio of 1.6 ppbv, where the dashed curve shows the effects of assuming 3.2 ppbv of odd chlorine. When the lower value of the odd chlorine mixing ratio is used, the model predictions for HCl are in agreement with the 15-to-20-km-altitude measurements of FARMER et al. (1976), ACKERMAN et al. (1976), WILLIAMS et al. (1976), and EYRE and ROSCOE (1977). However, the predicted HCl curves are a factor of two to three below the measurements of HCl at 25 km and above. Doubling the assumed odd-chlorine mixing ratio to 3.2 ppbv in the model brings the model predictions of HCl into better agreement with the HCl measurements above 25 km. (See Fig. 8.) However, an assumption of an asymptotic mixing ratio of at least 4 ppbv odd chlorine is needed to match the Cl and ClO measurements of ANDERSON et al. (1977) and MENZIES (1979). Although a model assumption of 3.2 ppbv of odd chlorine does not significantly change the overall agreement between the model predictions and the measurements of ozone, it does result in better agreement with the measurements of HCl above 20 km and with Cl and ClO.

Sensitivity of the comparisons to the assumed odd nitrogen abundance

To determine the sensitivity of the ozone comparison to the amount of odd nitrogen assumed to be present in the stratosphere, the model was run for two different assumptions about the background level of odd nitrogen. The model calculates 13 ppbv of odd nitrogen at 40-km altitude when simulating the ambient atmosphere. This result is nearly independent of the latitude but it does depend on the altitude. For the sensitivity test considered here, the odd-nitrogen mixing ratios at all latitudes and altitudes were multiplied by 1.5 and then the model was run for one simulated year. The 13 ppbv and the 18 ppbv of odd nitrogen used in this test are above the 11 ppbv measured by EVANS et al. (1976) and the 13 ppbv deduced by ACKERMAN et al. (1975), but they are below the odd-nitrogen abundance implied by the NO_2 measurement of HARRIES et al. (1976). The predicted effects of the increased odd nitrogen are shown in Fig. 9. An examination of this figure shows that the predicted effects are negligible at 1 mb and small at 2 mb, but substantial at 5 and 10 mb. That the predicted effects are more pronounced at lower altitudes than at higher altitudes shows that the destruction of ozone is dominated by odd-nitrogen reactions at the lower altitudes and by other (i.e., odd hydrogen) reactions at the upper altitudes. It is clear from the figure that changes in the model assumptions over this range of values can cause a 10% change in the predicted ozone abundance at 5 mb.

Sensitivity of the comparisons to the transport parameterization

Because the comparisons are at altitudes where ozone is close to photo-chemical equilibrium, the comparisons are not expected to be strongly influenced by the exact choice of the transport parameters. The dashed curves in

Fig. 10 shows comparisons for the case where both the winds and eddy transport were reduced by a factor of two. This reduces the ozone fluxes by a factor of two because neither the ozone abundances nor their gradients are appreciably changed. From this figure it can be seen that only minimial changes of the predictions at the 1- and 2-mb pressure heights occur except near the winter pole. However, significant improvements in the comparisons at the 5- and 10-mb heights are evident at both mid and high latitudes. In the polar regions, the agreement between the predictions and the observations is significantly enhanced by the reduction of the transport parameters. The substantial changes that occur at all altitudes near the winter pole show the importance of the transport parameterization when the ozone that is present is primarily that which has been transported from lower latitudes. In general, however, we can conclude that the comparisons at low and midlatitudes are, as expected, not highly sensitive to simple scaling changes in the transport parameters.

6. Summary

Model predictions of the variation of the ozone distribution with altitude, latitude, and season represent the state of our understanding of the mechanisms that control the production, loss, and movement of ozone. However, there are many uncertainties concerning the exact values of boundary conditions, input parameters, and the quantitative representation of transport, especially above balloon attitudes. Hence, the validation of atmospheric models is critical to developing the capability of predicting the impact of anthro-pomorphic activities. The present comparison between model predictions and BUV ozone observations has shown that the predicted variation of the latitude dependence with altitude and with season agrees well with the observed variations.

The sensitivity of the model predictions to uncertainites in the strato-
spheric temperatures, the abundance of water vapor, the abundance of odd
chlorine, the abundance of odd nitrogen, and the transport parameterization
was examined. The results of the sensitivity test indicate that:

1. A ±3°C temperature uncertainty contributes a ±5% change in the
predicted ozone abundances.

2. When the assumed stratospheric water-vapor mixing ratio is changed
from 4 ppmv to 8 ppmv, the model predictions change from 3% to 15%, depending
on both latitude and altitude.

3. A model assumption of an asymptotic mixing ratio of 3.2 ppbv for
odd chlorine lowers the predicted ozone abundance by 15% but does not
significantly change the overall agreement with the observed ozone abundances.

4. A 50% increase in the assumed odd-nitrogen level causes the pre-
dictions of the ozone abundance to decrease by 10% at 5 mb.

5. Although the model predictions of the ozone abundances at these
altitudes are not highly sensitive to the exact values of the transport para-
meters, the agreement between the predictions and the observations is
significantly improved at mid and high latitudes when the transport parameters
are reduced by a factor of two.

Photochemical Reaction Rates

Chemical reactions and corresponding rate coefficients

No.	Reaction	Rate coefficient[a]	Reference
1	$O + O_3 \rightarrow O_2 + O_2$	1.5×10^{-1} $exp(-2218/T)$	b
2	$O + O_2 + M \rightarrow O_3 + M$	1.1×10^{-34} $exp(510/T)$	c
3	$NO_2 + O \rightarrow NO + O_2$	9.3×10^{-12}	b
4	$NO + O_3 \rightarrow NO_2 + O_2$	2.3×10^{-12} $exp(-1450/T)$	b
5	$NO_3 + NO \rightarrow NO_2 + NO_2$	8.7×10^{-12}	c
6	$O_3 + NO_2 \rightarrow NO_3 + O_2$	1.2×10^{-13} $exp(-2450/T)$	d
7	$O(^1D) + M \rightarrow O + M$	1.659×10^{-11} $exp(107/T)$ $+ 0.58\ 10^{-11} exp(67/T)$	d
8	$O + OH \rightarrow H + O_2$	4.0×10^{-11}	b
9	$O_3 + H \rightarrow OH + O_2$	1.4×10^{-10} $exp(-470/T)$	b
10	$NO + O + M \rightarrow NO_2 + M$	1.55×10^{-32} $exp(584/T)$	d
11	$NO_2 + NO_3 + M \rightarrow N_2O_5 + M$	e	TURCO and WHITTEN (1975)
12	$O(^1D) + H_2O \rightarrow 2OH$	2.3×10^{-10}	d
13	$O_3 + HO_2 \rightarrow OH + O_2$	1.1×10^{-14} $exp(-580/T)$	ZAHNISER and HOWARD (1978)
14	$O + HO_2 \rightarrow OH + O_2$	3.5×10^{-11}	d
15	$NO_2 + OH + M \rightarrow HNO_3 + M$	f	d
16	$OH + HNO_3 \rightarrow H_2O + NO_3$	8.5×10^{-14}	b
17	$O + O + M \rightarrow O_2 + M$	$3 \times 10^{-33}(300/T)^3$	c
18	$OH + HO_2 \rightarrow H_2O + O_2$	4×10^{-11}	b
19	$OH + CO \rightarrow H + CO_2$	$1.35 \times 10^{-13}(1+P_{atm})$	b
20	$H + O_2 + M \rightarrow HO_2 + M$	2.1×10^{-32} $exp(290/T)$	d

See footnotes at end of table, p. 24 .

No.	Reaction	Rate coefficient[a]	Reference
21	$O + HNO_3 \rightarrow OH + NO_3$	1×10^{-14}	c
22	$OH + O_3 \rightarrow HO_2 + O_2$	$1.6 \times 10^{-12} \exp(-940/T)$	b
23	$NO + HO_2 \rightarrow NO_2 + OH$	$3.4 \times 10^{-12} \exp(250/T)$	b
24	$NO_2 + O + M \rightarrow NO_3 + M$	g	TURCO and WHITTEN (1975)
25	$N_2O_5 + M \rightarrow NO_2 + NO_3 + M$	h	TURCO and WHITTEN (1975)
26	$H + OH + M \rightarrow H_2O + M$	$6.1 \times 10^{-26} \, T^{-2}$	c
27	$N + O_3 \rightarrow NO + O_2$	$5 \times 10^{-12} \exp(-650/T)$	d
28	$N + NO \rightarrow N_2 + O$	3.4×10^{-11}	b
29	$N + O_2 \rightarrow NO + O$	$5.5 \times 10^{-12} \exp(-3220/T)$	d
30	$N + OH \rightarrow NO + H$	5.3×10^{-11}	c
31	$NO + OH + M \rightarrow HNO_2 + M$	$2.2 \times 10^{-32} \exp(1100/T)$	c
32	$OH + OH \rightarrow H_2O + O$	$1 \times 10^{-11} \exp(-500/T)$	b
33	$OH + HNO_2 \rightarrow H_2O + NO_2$	8×10^{-14}	c
34	$O(^1D) + N_2 + M \rightarrow N_2O + M$	3.5×10^{-37}	d
35	$O(^1D) + N_2O \rightarrow N_2 + O_2$	5.1×10^{-11}	b
36	$O(^1D) + N_2O \rightarrow NO + NO$	5.9×10^{-11}	b
37	$O + HNO_2 \rightarrow OH + NO_2$	1.5×10^{-14}	c
38	$OH + OH + M \rightarrow H_2O_2 + M$	$1.25 \times 10^{-32} \exp(900/T)$	d
39	$OH + H_2O_2 \rightarrow H_2O + HO_2$	$1 \times 10^{-11} \exp(-750/T)$	d
40	$HO_2 + HO_2 \rightarrow H_2O_2 + O_2$	2.5×10^{-12}	d
41	$O + H_2O_2 \rightarrow OH + HO_2$	$2.8 \times 10^{-12} \exp(-2125/T)$	b

No.	Reaction	Rate coefficient[a]	Reference
42	$HCl + OH \rightarrow H_2O + Cl$	$2.8 \times 10^{-12} \exp(-425/T)$	ZAHNISER et al. (1974)
			SMITH and ZELLER (1974)
			RAVISHANKARA et al. (1977)
43	$HCl + O \rightarrow OH + Cl$	$1.14 \times 10^{-11} \exp(-3370/T)$	b
44	$Cl + CH_4 \rightarrow HCl + CH_3$	$9.9 \times 10^{-12} \exp(-1359/T)$	b
45	$Cl + H_2 \rightarrow HCl + H$	$3.5 \times 10^{-11} \exp(-2290/T)$	d
46	$Cl + O_3 \rightarrow ClO + O_2$	$2.8 \times 10^{-11} \exp(-257/T)$	b
47	$ClO + O \rightarrow Cl + O_2$	$7.7 \times 10^{-11} \exp(-130/T)$	d
48	$ClO + NO \rightarrow Cl + NO_2$	$7.8 \times 10^{-12} \exp(250/T)$	b
49	$ClO + CO \rightarrow Cl + CO$	1.7×10^{-15}	c
50	$ClO + NO_2 + M \rightarrow ClONO_2 + M$	i	d
51	$ClONO_2 + O \rightarrow ClO + NO_3$	$3 \times 10^{-12} \exp(-808/T)$	b
52	$Cl + HO_2 \rightarrow HCl + O_2$	4.5×10^{-11}	b
53	$O(^1D) + H_2 \rightarrow OH + H$	9.9×10^{-11}	d
54	$O(^1D) + CH_4 \rightarrow OH + CH_3$	1.3×10^{-10}	d
55	$OH + CH_4 \rightarrow H_2O + CH_3$	$2.4 \times 10^{-12} \exp(-1710/T)$	b
56	$CH_3 + O_2 + M \rightarrow CH_3O_2 + M$	j	TURCO and WHITTEN (1975)
57	$CH_3 + O \rightarrow CH_2O + H$	1.2×10^{-10}	k
58	$2CH_3O_2 \rightarrow 2CH_3O + O_2$	2.0×10^{-15}	k
59	$CH_3O_2 + NO \rightarrow CH_3O + NO_2$	8×10^{-12}	b
60	$CH_3O_2 + HO_2 \rightarrow CH_4O_2 + O_2$	1×10^{-12}	b
61	$CH_4O_2 + OH \rightarrow CH_3O_2 + H_2O$	$6.2 \times 10^{-12} \exp(-750/T)$	b

No.	Reaction	Rate coefficient[a]		Reference
62	$CH_3O + O_2 \rightarrow CH_2O + HO_2$	$5 \times 10^{-13} \exp(-2000/T)$	b	
63	$CH_2O + O \rightarrow CHO + OH$	$2.8 \times 10^{-11} \exp(-1540/T)$	b	
64	$CH_2O + OH \rightarrow CHO + H_2O$	$1.7 \times 10^{-11} \exp(-100/T)$	b	
65	$CHO + O_2 \rightarrow CO + HO_2$	5×10^{-12}	b	
66	$CHO + O \rightarrow CO + OH$	1.0×10^{-10}	k	
67	$CHO + O \rightarrow CO_2 + H$	7.0×10^{-11}	k	
68	$CH_3CL + OH \rightarrow H_2O + CH_2O + CLO$	$2.? \times 10^{-12} \exp(-1142/T)$	b	
69	$CH_2O + CL \rightarrow HCL + CHO$	7.5×10^{-11}	b	

Photodissociation Rates

No.	Reaction	Dissociation rate[1]	References
J_1	$O_2 + h\nu \rightarrow 2O(^3P)$	9.7×10^{-6}	HUDSON and MAHLE (1972); OGAWA (1968); BLAKE et al. (1966); WATANABE et al. (1953)
J_2	$O_3 + h\nu \rightarrow O_2 + O(^3P)$	3.47×10^{-4}	INN and TANAKA (1953); GRIGGS (1968); JONES and WAYNE (1969)
J_3	$O_3 + h\nu \rightarrow O_2 + O(^1D)$	5.06×10^{-3}	INN and TANAKA (1953); GRIGGS (1968); JONES and WAYNE (1969)
J_4	$NO + h\nu \rightarrow N + O$	2.78×10^{-6}	CIESLIK and NICOLET (1973)
J_5	$NO_2 + h\nu \rightarrow NO + O$	5.88×10^{-3}	HALL and BLACET (1952); NAKAYAMA et al. (1959); PITTS et al. (1964)

See footnotes at end of table, p. 24.

No.	Reaction	Dissociation rate[1]	References
J_6	$H_2O + h\nu \rightarrow OH + H$	1.6×10^{-8}	WATANABE and ZELIKOFF (1953)
J_7	$HNO_3 + h\nu \rightarrow NO_2 + OH$	7.17×10^{-5}	JOHNSTON and GRAHAM (1974)
J_8	$HNO_2 + h\nu \rightarrow NO + OH$	4.29×10^{-4}	JOHNSTON and GRAHAM (1972)
J_9	$N_2O + h\nu \rightarrow N_2 + O(^1D)$	4.54×10^{-7}	JOHNSTON and SELWYN (1975)
J_{10}	$NO_3 + h\nu \rightarrow NO_2 + O \rightarrow NO + O_2$	1.66×10^{-2} 2.66×10^{-2}	JOHNSTON and GRAHAM (1974)
J_{11}	$N_2O_5 + h\nu \rightarrow 2NO_2 + O$	3.84×10^{-4}	GRAHAM (1975)
J_{12}	$HO_2 + h\nu \rightarrow OH + O$	5.43×10^{-4}	PAUKERT and JOHNSTON (1973)
J_{13}	$H_2O_2 + h\nu \rightarrow 2OH$	7.64×10^{-5}	MOLINA et al. (1977)
J_{14}	$HCl + h\nu \rightarrow H + Cl$	5.65×10^{-6}	MYER and SAMSON (1970)
J_{15}	$ClO + h\nu \rightarrow Cl + O$	3.36×10^{-3}	JOHNSTON et al. (1969); LANGHOFF et al. (1977)
J_{16}	$ClONO_2 + h\nu \rightarrow ClO + NO_2$	3.52×10^{-4}	b
J_{17}	$CF_2Cl_2 + h\nu \rightarrow 2Cl$	9.92×10^{-7}	a
J_{18}	$CFCl_3 + h\nu \rightarrow 2.5Cl$	6.27×10^{-6}	a
J_{19}	$CH_2O + h\nu \rightarrow CHO + H$	5.0×10^{-5}	TURCO (1975)
J_{20}	$CH_2O + h\nu \rightarrow CO + H_2$	7.0×10^{-5}	TURCO (1975)
J_{21}	$CH_4O_2 + h\nu \rightarrow CH_3O + OH$		
J_{22}	$CH_3Cl + h\nu \rightarrow CH_3 + Cl$	1.05×10^{-7}	ROBBINS (1976)

[a] In units of cm^3 sec^{-1} for bimolecular reactions and cm^6 sec^{-1} for trimolecular reactions.

[b] NASA Panel for Data Evaluation, 1979.

^{c}Rate coefficients are those recommended in HAMPSON and GARVIN (1975).

^{d}Rate coefficients are the values recommended in HUDSON (1777). See Table 1 in HUDSON (1977) and corresponding notes therein for a discussion of the pertinent laboratory measurements upon which these values are based.

^{e}The three-body reaction-rate coefficient:

$k_{11} = (1.9 \times 10^{-30})/(1 + 5V_o) \cdot (3 + 5V_o)/(3 + V_o)$ cm^6 sec^{-1}, where $V_o = 5 \times 10^{-19}$[M].

^{f}The equivalent three-body reaction-rate coefficient for the formation of HNO$_3$ is given by: $k_{16} = (0.94/M)(280/T)^{1/2} 10^{-AT/(B+T)}$ cm^6 sec^{-1}, where:

$A = 31.62273 - 0.258304 \cdot Z - 0.0889287 \cdot Z^2 + 2.520173 \times 10^{-3} \cdot Z^3$

$B = -327.372 + 44.5586 \cdot Z - 1.38092 \cdot Z^2$

$Z = \log_{10}[0.78 \cdot M]$

$T = $ temperature

^{g}The reaction-rate coefficient k_{24} is given by

$k_{24} = 2.8 \times 10^{-31}/(1 + 2.55 \times 10^{-20}$ M) cm^6 sec^{-1}.

^{h}The reaction-rate coefficient for the collisional destruction of N$_2$O$_5$ is given by $k_{25} = 2.2 \times 10^{-5} V_o(4 + V_1)/[(1 + V_1)(4 + V_1/6)]$, where $V_o = \exp(-9700/T)$ and $V_1 = 2.3 \times 10^{-19} \exp(900/T)$ M.

^{i}The formation rate of chlorine nitrate is given by:

$k_{50} = 3.3 \times 10^{-23} T^{-3.34}/(1 + 8.7 \times 10^{-9} T^{-0.6} M^{0.5})$ cm^6 sec^{-1}.

^{j}The pressure-dependent three-body reaction-rate coefficient is

$k_{56} = 2.6 \times 10^{-31}/(1 + 6.047 \times 10^{-19} \cdot M)$.

^{k}See POPPOFF et al. (1978) for reference list and detailed discussion of the methane oxidation cycle.

^{l}Photodissociation rates represent diurnally averaged values (altitude 60 km, latitude 45° N, Autumn). The units are sec^{-1}.

[m]Reaction rates are calculated from the cross sections tabulated in HUDSON (1977).

[n]Since no photodissociation cross sections are available at the time of writing, we have assumed (after TURCO and WHITTEN, 1975) that the dissociation rate of CH_4O_2 is comparable to that of H_2O_2.

References

ACKERMAN, M., FONTANELLA, J. C., FRIMONT, D., GIRAND, A., LOUISNARD, N., and MULLER, C. (1975), Simultaneous measurements of NO and NO_2 in the stratosphere, Planet Space Sci. 23, 651-660.

ACKERMAN, M., FRIMONT, D., GIRARD, A., GATTIGNIES, M., and MULLER C. (1976), Stratospheric HCl from infrared spectra, Geophys. Res. Let. 3, 81-83.

ANDERSON, J. G., MARGITAN, J. J., and STEDMAN, D. M. (1977), Atomic chlorine and the chlorine monoxide radical in the stratosphere, Science 198, 501-503.

BARNETT, J. J. (1974) The mean meriodional temperature behaviour of the stratosphere from November 1970 to November 1971 derived from measurements by the Selective Chopper Radiometer on Nimbus IV, Quart. J. Royl. Meteorol. Soc. 100, 505-530.

BLAKE, A. J., CARVER, J. H., and HADDAD, G. N. (1966), Absorption cross sections of molecular oxygen between 1250 A and 2350 A, J. Quant. Spect. Rad. Trans. 6, 451.

CHURCHILL, R. V. (1958) Operational Mathematics, New York, McGraw-Hill.

CIESLIK, S. and NICOLET, M. (1973), The aeronomic dissociation of nitric oxide, Planetary and Space Sci. 21, 925.

COWLEY, A. C., and BORUCKI, W. J. (1976), Exponential approximation for daily average solar heating or photolysis, J. Atmos. Sci. 33, 1347-1356.

CUNNOLD, D., ALYEA, F., PHILLIPS, N., and PRINN, R. (1975), A three-dimensional dynamical-chemical model of atmospheric ozone, J. Atmos. Sci. 32, 170-194.

EVANS, W. F. J., KERR, J. B., WARDLE, D. I., McCONNELL, J. C., RIDLEY, B. A., and SCHIFF, M. I. (1976), Intercomparison of NO, NO$_2$, and HNO$_3$ measurements with photochemical theory, Atmosphere 14, 189-198.

EYRE, J. R., and ROSCOE, H. K. (1977), Radiometric measurement of stratospheric HCl, Nature 266, 243-244.

FARMER, C. B., RAPER, O. F., and NORTON, R. (1976), Spectroscopic detection and vertical distribution of HCl in the troposphere and lower stratosphere, Geophys. Res. Let. 3, 13-16.

FLEIG, A. (1980) Personal communication, Goddard Space Flight Center, Greenbelt Md.

FREDHOLM (1900), Ofversigt at K. Ventenskaps-Akad. Förhandlingar (Stockholm), LVII, pp. 39-46.

GRAHAM, R. A. (1975), Photochemistry of NO$_3$ and the kinetics of the N$_2$O$_5$-O$_3$ system, Ph.D. dissertation, University of California, Berkeley, California.

GREEN, A. E. S. (1964), Attenuation by ozone and the Earth's albedo in the middle ultraviolet, Appl. Opt., 3, 203-208.

GRIGGS, M. (1968), Absorption coefficients of ozone in the ultraviolet and visible regions, J. Chem. Phys. 49, 857.

HALL, T. C., and BLACET, F. E. (1952), Separation of the absorption spectra of NO$_2$ and N$_2$O$_4$ in the range of 2400-5000 A, J. Chem. Phys. 30, 1745.

HAMPSON, F. R., and GARVIN, D. (1975), Chemical kinetic and photochemical data for modeling atmospheric chemistry, National Bureau of Standards Technical Note 866, Supt. of Doc., U.S. Government Printing Office, Washington, D.C., 20402.

HARRIES, J. E., MOSS, D. G., SWANN, N. R. W., NEILL, G. F., and GILDWANG, P. (1976), Simultaneous measurements of H_2O, NO_2, and HNO_3 in the daytime stratosphere from 15 to 35 km, Nature 259, 300-302.

HEATH, D. F. (1979), Spectrometric calibration and operating characteristics in space of the BUV experiment on Nimbus 4 and SBUV/TOMS experiment on Nimbus 7, submitted to Applied Optics.

HEATH, D. F., MATEER, C. L., and KRUEGER, A. J. (1973), The Nimbus-4 backscatter ultraviolet (BUV) atmospheric ozone experiment-two years' operation, Pure and Appl. Geophys. (PAGEOPH) 106-108, 1238-1225.

HILSENRATH, E. GUENTHER, B., and DUNN, P. (1977), Water vapor in the lower stratosphere measured from aircraft flight, JGR 82, 5453-5458.

HUDSON, R. D., ed. (1977) Chlorofluoromethanes and the stratosphere, NASA Reference Publication 1010, Supt. of Doc., U.S. Government Printing Office, Washington, D.C., 20402.

HUDSON, R. D., ed. (1980), User's Manual for BUV Data, to be published in 1980.

HUDSON, R. D., and MAHLE, S. H. (1972), Photodissociation rates of molecular oxygen in the mesosphere and lower thermosphere, J. Geophys. Res. 77, 2902-2914.

INN, E. C. Y., and TANAKA, Y. (1953), Absorption coefficient of ozone in the ultraviolet and visible regions, J. Am. Opt. Soc. 43, 870-873.

JOHNSTON, M. S., KATTERHNORN, D., and WHITTEN, G. (1976), Use of excess carbon 14 data to calibrate models of stratosphere ozone depletion by supersonic transports, JGR 81, 368-380.

JOHNSTON, H. S., and GRAHAM, R. (1972), Photochemistry of NO_x and HNO_x compounds, J. Phys. Chem. 77, 62.

JOHNSTON, H. S., and CRAHAM, R. (1974), Gas-phase ultraviolet absorption spectrum of nitric acid vapor, Can. J. Chem. 52, 8.

JOHNSTON, H. S., MORRIS, E. D., and VAN den BOGAERDE, J. E., (1969), Molecular modulation kinetic spectrometry. ClOO and ClO_2 radicals in the photolysis of chlorine in oxygen, J. Am. Chem. Soc. 91, 7712.

JOHNSTON, H. S., and SELWYN, C. S. (1975), New cross sections for the absorption of near ultraviolet radiation by nitrous oxidy (N_2O), Geophys. Res. Let. 2, 549.

JONES, I. T. N., and WAYNE, R. P. (1969), Photolysis of ozone by 254-, 313-, and 334-nm radiation, J. Chem. Phys. 51, 3617.

LANGHOFF, S. R., JAFFE, R. L., and ARNOLD J. O. (1977), Effective cross sections and rate constants for predissociation of ClO in the Earth's atmosphere, JQSRT, 18, 227.

LUTHER, F. M., and GELINAS, R. J. (1976) Effect of molecular multiple scattering and surface albedo on atmospheric photo-dissociation rates, J. Geophys. Res. 81, 1125-1132.

MATEER, C. L. (1972) "Mathematics of Profile Inversion," A Review of Some Aspects of Inferring the Ozone Profile by Inversion of Ultraviolet Radiance Measurements, edited by Lawrence Colin. NASA TMX-62,150, 1972, pp. 1-2 to 1-25.

MENZIES, R. T. (1979), Remote measurements of ClO in the stratosphere, Geophys. Res. Let. 6, 151-153.

MOLINA, LUISA T., SCHINKE, STANLEY D. AND MOLINA, MARIO, J. (1977), Ultraviolet absorption spectrum of hydrogen peroxide vapor, Geophys. Res. Let. 4, No. 12, 580-582.

MYER, J. A., and SAMSON, J. A. (1970), <u>Vacuum-ult.aviolet absorption cross</u> <u>sections of CO, HCl, and ICN between 1050 and 2100 A</u>, J. Chem. Phys. <u>52</u>, 266.

NAKAYAMA, T., KITAMURA, M. Y., and WATANABE, K. (1959), <u>Ionization potential</u> <u>and absorption coefficients of nitrogen dioxide</u>, J. Chem. Phys. <u>30</u>, 1180.

NASTROM, G. D., and BELMONT, A. D. (1975) <u>Periodic variations in stratospheric-</u> <u>mesospheric temperature from 20-65 km at 80° N to 30° S</u>, J. Atmos. Sci. <u>32</u>, 1715-1722.

NASA Panel for Data Evaluation (1979), <u>Chemical Kinetic and Photochemical</u> <u>Data for Use in Stratospheric Modeling; Evaluation Number 2</u>, JPL Publication 79-127 (NASA CR-158514).

OGAWA, M. (1968), <u>Absorption coefficients of O_2 at the Lyman-line and its</u> <u>vicinity</u>, J. Geophys. Res. <u>73</u>, 6759.

OORT, A. H., and RASMUSSEN, E. M. (1971), <u>Atmospheric circulation statistics</u>, NOAA Professional Paper 5.

PAUKERT, T. T., and JOHNSTON, H. S. (1973), <u>Spectra and kinetics of the hydro-</u> <u>peroxyl free radical in the gas phase</u>, J. Chem. Phys. <u>56</u>, 2824.

PHILLIPS, D. (1962), <u>A technique for the numerical solution of certain</u> <u>integral equations of the first kind</u>, J. Assoc. Comp. Mach <u>9</u>, 84-97.

PITTS, J. N., SHARP, J. H., and CHAN, S. I. (1964), <u>Effects of wavelength and</u> <u>temperature on primary processes in the photolysis of nitrogen dioxide and</u> <u>a spectroscopic-photochemical determination of the dissociation energy</u>, J. Chem. Phys. <u>40</u>, 3655.

POPPOFF, I. G., WHITTEN, R. C., TURCO, R. P., and CAPONE, L. A. (1978), <u>An</u> <u>assessment of the effect of supersonic aircraft operations on the strato-</u> <u>spheric ozone content</u>, NASA Reference Publication <u>1026</u>, Supt. of Doc., U.S. Government Printing Office, Washington, D.C., 20402.

PRABHAKARA, C., RODGERS, E. B., and SALOMANSON, V. V. (1973), Remote sensing of global distribution of total ozone and the infrared upper-tropospheric circulation from Nimbus IRIS experiments, Pure and Appl. Geophys. 106-108, 1226.

RAPER, O. F., FARMER, C. B. TOTH, R. A., and ROBBINS, D. B. (1977), The vertical distribution of HCl in the stratosphere, GRL 4, 531-534.

RAVISHANKARA, A. R., SMITH, G., WATSON, R. T., and DAVIS, D. D. (1977), A temperature dependent kinetics study of the reactions of HCl with OH and $O(^3\Gamma)$, J. Phys. Chem. 51, 2220-2225.

ROBBINS, D. E. (1976), Photodissociation of methyl chloride and methyl bromide in the atmosphere, GRL 3, 213-216.

TURCO, R. P. (1975), Photodissociation rates in the atmosphere below 100 km, Geophys. Surveys 2, 153-192.

TURCO, R. P., and WHITTEN, R. C. (1975), Chloroflouromethanes in the stratosphere and some possible consequences for ozone, Atmos. Env. 9, 1045-1061.

TURCO, R. P., and WHITTEN R. C. (1978), A note on the diurnal averging of aeronomical models, J. Atmos. Terr. Phys. 40, 13-20.

TWOMEY, S. (1961), On the deduction of the vertical distribution of ozone by ultraviolet spectral measurements from a satellite, J. Geophys. Res. 66, 2153-2162.

TWOMEY, S. (1963), On the numerical solution of Fredholm integral equations of the first kind by the inversion of the linear system produced by quadrature, J. Assoc. Comp. Mach. 10, 97-101.

WATANABE, K., INN, E. C. Y., and ZELIKOFF, M. (1953), Absorption coefficients of oxygen in the vacuum ultraviolet, J. Chem. Phys. 21, 1026.

WATANABE, K., and ZELIKOFF, M. (1953), Absorption coefficients of water vapor in the vacuum ultraviolet, J. Am. Opt. Soc. 43, 753.

WHITTAKER, E. T. and WATSON, G. N. (1958), A Course in Modern Analysis, Cambridge, England, The University Press.

WHITTEN, R. C., BORUCKI, W. J., WATSON, V. R., SHIMAZAKI, T., WOODWARD, H. T., RIEGEL, C. A., CAPONE, L. A., and BECKER, T. (1977), The NASA-Ames Research Center one- and two-dimensional stratospheric models. II. The two-dimensional model, NASA Technical Paper 1003. Supt. of Doc., U.S. Government Printing Office, Washington, D.C., 20402.

WILCOX, R. W., NASTROM, G. D., and BELMONT, A. D. (1977), Periodic variations of total ozone and of its vertical distribution, J. Appl. Met. 16, 290-298.

WILLIAMS, W. J., KOSTUS, J. J., GOLDMAN, A., and MURCRAY, D. G. (1976), Measurements of the stratosphere mixing ratio of HCl using infrared absorption technique, Geophys. Res. Let. 3, 383-385.

ZAHNISER, M. S., KAUFMAN, F., and ANDERSON, J. G. (1974), Kinetics of the reaction of OH with HCl, Chem. Phys. Let. 27, 507-510.

ZAHNISER, M. S., and HOWARD, C. J. (1978), Direct measurement of the temperature dependence of the rate constant for the reaction $HO_2 + O_3 \xrightarrow{k_1} OH + 2O_2$ 4th Biennial Rocky Mountain Regional Meeting, American Chemical Society, Boulder, Colorado.

Figure Captions

1. Schematic diagram of the BUV experiment.

2. Effective scattering levels for solar radiation in the nadir direction of the satellite for all orders of scattering; solar zenith angle = 60° and total ozone = 336 m atm-cm. (From HEATH et al., 1973.)

3. Comparison of the Goddard BUV observations with the Ames two-dimensional-model predictions for fall and winter. The symbols represent the BUV data for 1970 and 1971 while the solid curve represents the model predictions.

4. Comparisons of the Goddard BUV observations with the Ames two-dimensional-model predictions for spring and summer. The symbols represent the BUV data for 1970 and 1971 while the solid curve represents the model predictions.

5. Comparison of the model predictions and BUV data where the model temperatures are increased by 10°C.

6. Comparison of the model predictions and the BUV data when the water vapor mixing ratio in the model is changed from 4 ppmv to 8 ppmv.

7. Comparison of the model predictions and the BUV data when the odd-chlorine mixing ratio in the model is changed from 1.6 ppbv to 3.2 ppbv.

8. Comparison of the predicted and measured HCl abundance in the fall when an odd-chlorine asymptotic mixing ratio of 3.2 ppbv is assumed.

9. Comparison of the model predictions and the BUV data when the odd-nitrogen mixing ratio in the model is multiplied by 1.5.

10. Comparison of the model predictions and the BUV data when the model transport parameters are divided by two.
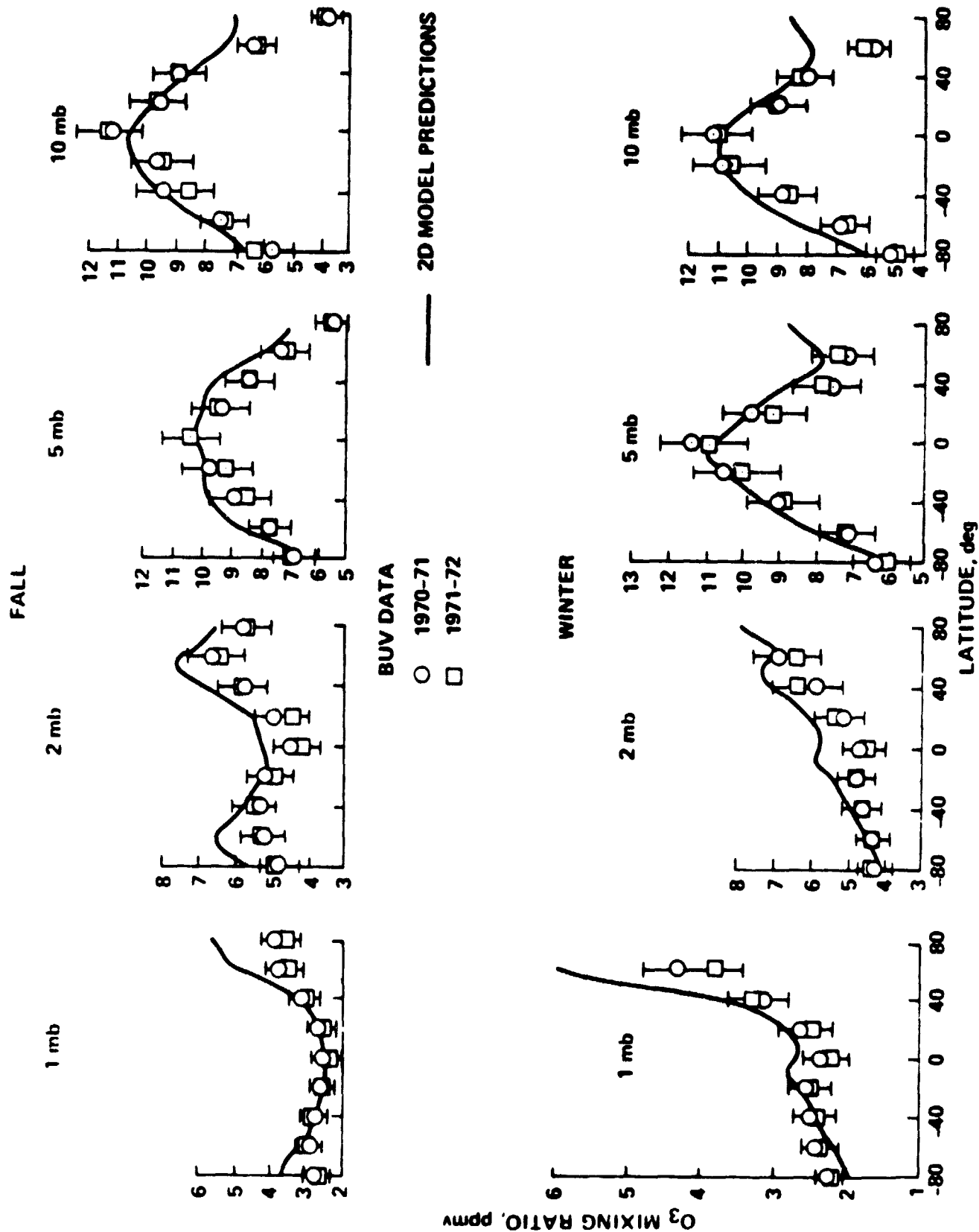
33

Fig. 1

SUNLIGHT

F_0

NIMBUS

Θ

OZONE ABSORPTION REGIME

SCATTERING LAYER

$I = I (\Omega, \Theta, R, \lambda)$ EARTH RADIANCE

$F_0 = F (\lambda)$ SOLAR IRRADIANCE

34

Fig. 2

Fig. 3

Fig. 4

37

Fig. 5

FIG. 6

Fig. 7

40

Fig. 8

WINTER

SPRING

2D MODEL PREDICTIONS
—— STANDARD CASE
—— 1.5 × ODD NITROGEN

BUV DATA
○ 1970–71
□ 1971–72

O₃ MIXING RATIO, ppmv

LATITUDE, deg

Fig. 9

SPRING

SUMMER

BUV DATA

O 1970-71
□ 1971-72

—— STANDARD CASE
- - - TRANSPORT RATE = ½ OF
THE STANDARD CASE

O₃ MIXING RATIO, ppmw

LATITUDE, deg

FIG. 10

43